Supplementary Methods

Whole Body Plethysmography

Ventilatory function was assessed by whole body plethysmography under unrestrained conditions (Buxco Research System). Each animal was acclimatized in a cylindrical chamber (200 ml) continuously ventilated with humidified air (350 ml/min) for at least 20 min before ventilation measurements were obtained. Chamber temperature was maintained within 25° C for adults and 30° C for neonates and was recorded with each measurement using a thermocouple device. In some experiments, normoxic/normocapnic air was replaced by hypercapnic air (CO_2 5%), or hypoxic air (O_2 10%) for 5 min. At constant chamber volume, changes in pressure because of inspiration and expiration were measured using a differential pressure transducer (Buxco Research System), amplified and digitally recorded. We measured the respiratory frequency (fR, in cycle per min, $c.min^{-1}$), the tidal volume (V_T, µl) normalized as the ratio V_T divided by the body weight (V_T, $\mu l.g^{-1}$), the minute ventilation (V_E, $ml.g^{-1}.min^{-1}$), the number of apneas per min > two normal respiratory cycles (apneas > $2T_{TOT}$) expressed as the Apnea Index (AI) and the irregularity score (IS, variability in duration of respiratory cycles, see Viemari et al., 2005) during 5 successive periods. Measurements were performed during: 1) control period under air, prior to the challenge, 2-3) the 3rd min and the 5th min of the challenge, 4) the post-challenge period (the first 2 min after the end of the challenge when normoxia or normocapnia were restored in the plethysmographic chamber), and 5) 10 to15 min later.

Electrophysiology

The brain stem was dissected in ice-cold artificial cerebral spinal fluid (ACSF) that was equilibrated with carbogen (95% O_2-5% CO_2, pH 7.4). Rhythmic slice preparations containing the preBötC were obtained by slicing the medulla using a microslicer (VT1000S; Leica). Slices

were submerged in a recording chamber (6 ml) under circulating ACSF (30°C; flow rate 18 ml/min, total circulating volume = 100 ml). ACSF contained (in mM): 118 NaCl, 3 KCl, 1.5 $CaCl_2$, 1 $MgCl_2 \cdot 6H_2O$, 25 $NaHCO_3$, 1 NaH_2PO_4, and 30 D-glucose, equilibrated with carbogen (95% O_2-5% CO_2, pH 7.4). Extracellular KCl was elevated from 3 to 8 mM over a span of 30 min before commencing recordings, to maintain rhythmic population activity.

Extracellular recordings were obtained with glass suction electrodes positioned on the slice surface in the ventral respiratory group (VRG) near or on top of the preBötC. The VRG population bursting is dominated by inspiratory neurons such that integrated VRG (int-VRG) activity is in-phase with integrated hypoglossal activity. Thus VRG population bursts serve as a marker of fictive inspiration. This population activity was rectified and integrated and the data were digitized with a Digidata acquisition system (Molecular Devices), stored on a PC using pClamp 10 (Molecular Devices) software, and analyzed off-line using pClamp 10. The int-VRG population burst amplitude was measured as baseline to peak height, whereas frequency was calculated based on the burst intervals. To minimize the potential influence of baseline fluctuations and differences in burst peak trajectories, the int. VRG burst duration was calculated as the duration of the burst at half-maximal burst amplitude.

Intracellular patch-clamp recordings were obtained with a MultiClamp 700B amplifier (Molecular Devices), using blind-patch technique to VRG neurons in 600- to 650-µm brain stem slice preparations. Patch electrodes were manufactured from filamented borosilicate glass tubes (Clark G150F-4; Warner Instruments) and filled with an intracellular solution containing (in mM): 140 K-gluconic acid, 1 $CaCl_2$, 10 EGTA, 2 $MgCl_2$, 4 ATP, and 10 HEPES.

Only inspiratory VRG neurons active in-phase with the int-VRG population burst were recorded in this study. The discharge pattern of each cell type was first identified in the cell-

attached mode and remained similar in whole cell configuration. Experiments were then performed in the whole cell patch-clamp mode.

In all experiments, the fictive inspiration was recorded for 20 min to get a control baseline. Then the gas (95% O_2 – 5% CO_2) bubbling ACSF was replaced by a mixture of 95% N_2 – 5% CO_2 (anoxia) for 10 minutes to test the response to decreased levels of O_2. A small percentage of ambient O_2 can diffuse in the solution (27); therefore this condition was labeled as hypoxia. In some experiments, 2 slices (1 from a KO or NesKO and one from a CT mouse) were put in the same bath and recorded at the same time to confirm the different responses observed between genotypes when exposed to the same conditions. The same statistical analyses as described for plethysmography recordings were applied to these data.

Histology

Free-floating sections (30 µm) were used for immunofluorescence. After blocking, sections were incubated O/N at 4ºC with antibodies against Iba1 (#019-19741, Wako, Japan 1:1000), GFAP (#G3893, Sigma, 1:1000), NK1R (#AB5060, Millipore, 1:500), CD11b (#MCA711, Abd Serotec 1:500) or Phox2B (1:1000, provided by Dr. Brunet, ENS Paris, France) and visualized using a corresponding fluorochrome-coupled secondary antibody (1:200, Jackson Immunoresearch).

Supplementary data

Supplementary Video 1. KO Mice Have Abnormal Breathing Activity

P22 KO mouse recorded during irregular breathing episode punctuated by distinct gasping events. This mouse was still in process of losing its hair, weighed 9 g, had a body temperature of 36.3º C, and was in the pre-symptomatic stage of disease progression.

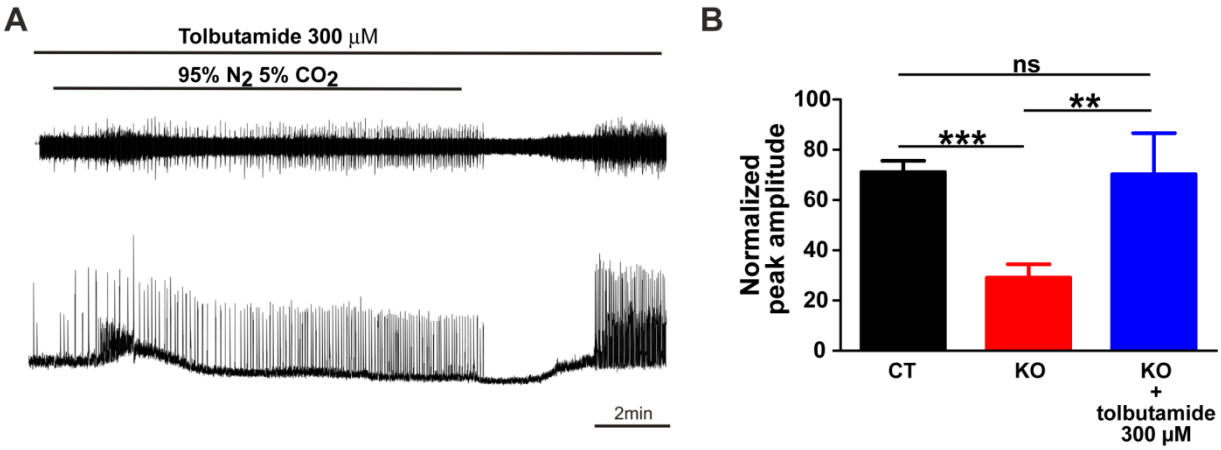

Supplementary Figure 1. Blockade of K_{ATP} channels restores fictive gasping in slices of KO mice.

(A) Multi unit population recordings (upper trace, integrated and rectified multi-unit recording ventral respiratory group (VRG) containing the PreBötC from brainstem slices of KO with Tolbutamide (300µM) in the bath in response to hypoxic conditions (95%N_2/5%CO_2). (B) Bath application of Tolbutamide (300 µM) restored the amplitude of fictive gasping in slices of KO mice (n=4) to levels observed in CT mice (n=10) and had significantly higher amplitudes compared to the slices of KO with no drug in the bath (n=10). ** p<0.01, ***p<0.001 vs CT mice (One-way ANOVA, Tukey post-hoc test).

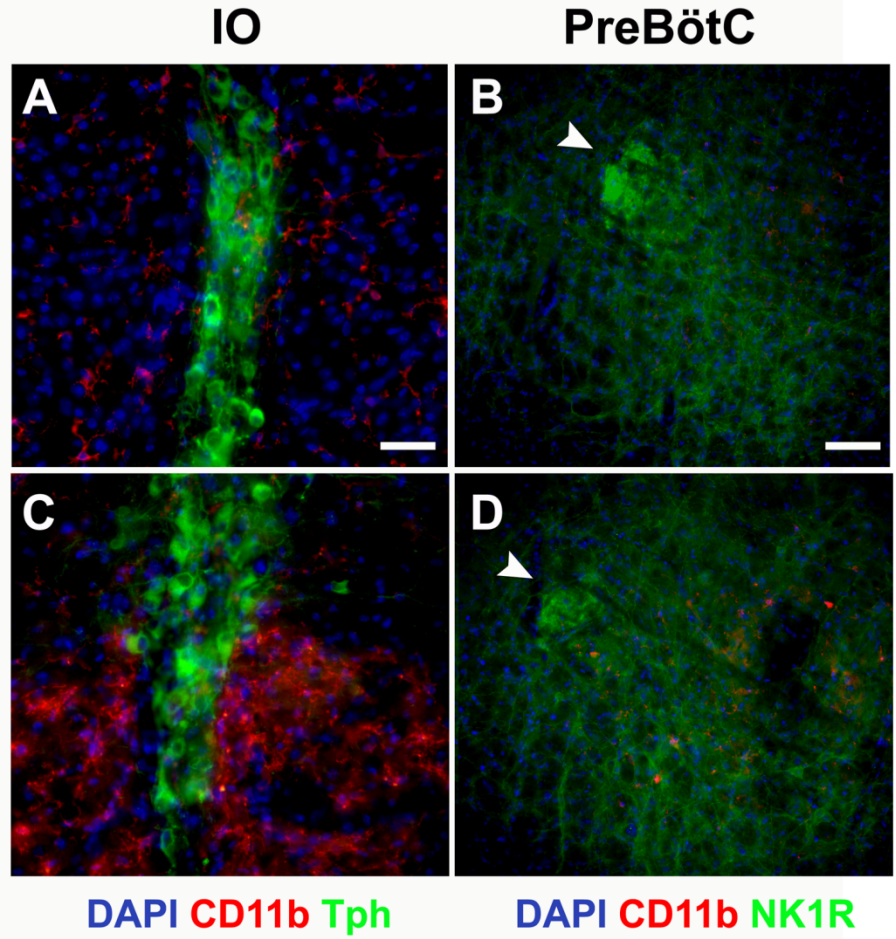

Supplementary Figure 2. Diverse degree of microglial activation in the ventral midline Raphe and the PreBötzinger complex in the ventrolateral medulla of KO mice

(A) No microglial activation is visible in the vicinity of serotoninergic (Tph positive) neurons in the ventral midline raphe of CT mice was determined using an antibody against CD11b in coronal sections (n=5). (B) Absence of CD11b staining in the PreBötzinger Complex (NK1R positive) neurons ventral to the Nucleus Ambiguus (arrowhead) of CT mice. (C) Overt microglial activation is observed around ventral Raphe serotoninergic neurons in late-stage KO mice (n=5). (D) Mild microgliosis is detected in the vicinity of the PreBötzinger complex (ventral to Nucleus Ambiguus, arrowhead) of late-stage KO mice. Scale bar A,C=12.5 μm; B,D=25 μm

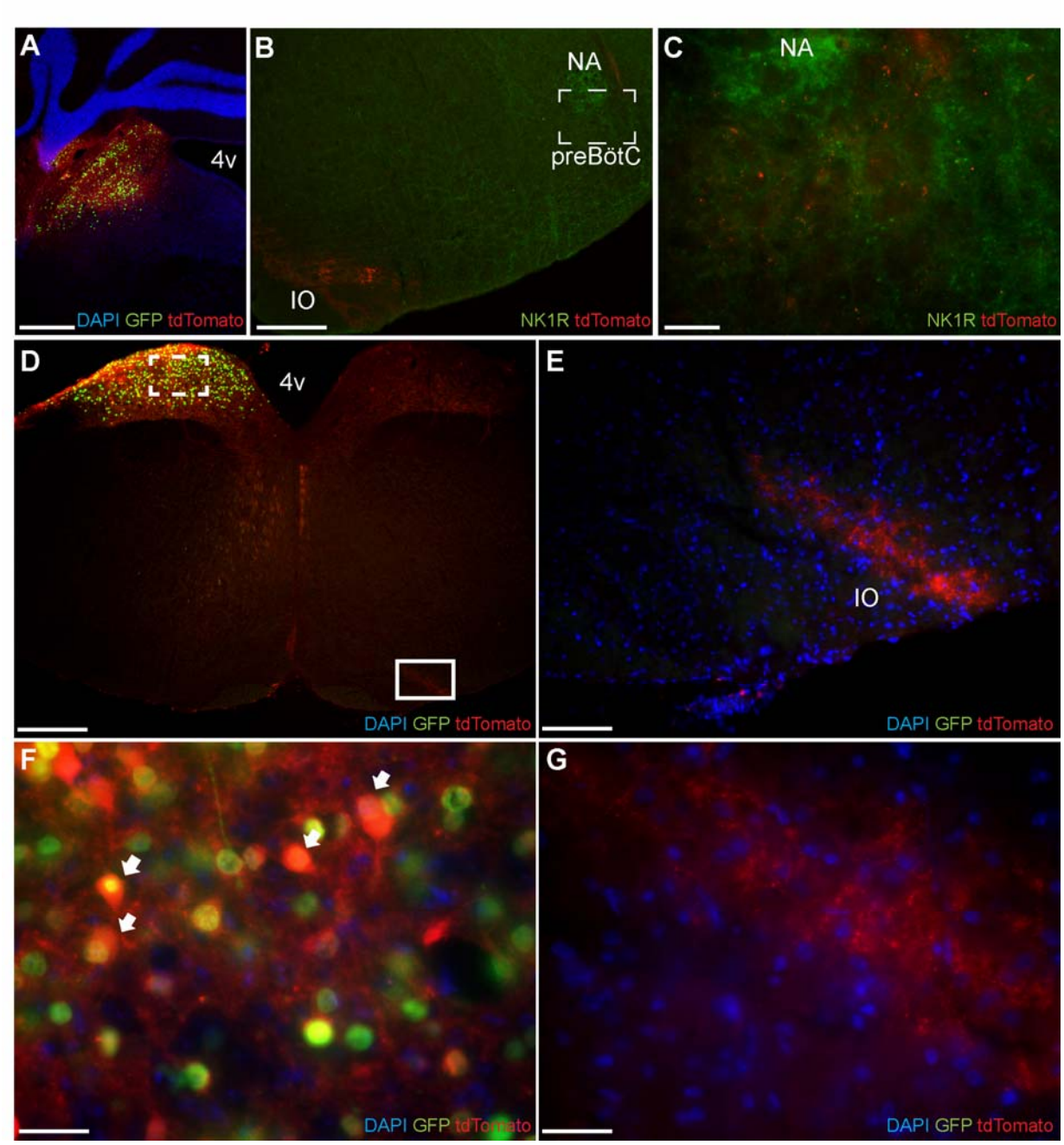

Supplementary Figure 3. VN neurons project to Inferior Olive and the preBötC region

(A) An AAV-CRE-GFP vector was injected in the VN of conditional tdTomato reporter mice (Ai14, Madison et al., 2010). Extensive GFP and tdTomato expression was observed in transduced cells. 4v:4th ventricle. Scale bar: 500 µm. Prominent tdTomato expression was observed in the inferior olive (IO) of VN-injected mice (B). Several terminal boutons were detected in the vicinity of the preBötzinger Complex (preBötC), defined as a NK1R-positive region ventral to the Nucleus Ambiguus (NA). (C) High magnification of the boxed area in panel B. Scale bars: B: 250 µm, C: 50 µm. (D-G) AAV-mediated cell transduction is restricted to the VN. (D) Extensive GFP expression was only observed in the injected area (dorsal medulla) Scale bar 500 µm. (E) TdTomato expression, but absence of GFP positive cells, is observed in

projection areas (IO). Scale bar 125 µm. (F-G) High magnification images of the transduced area (F, open box in C) shows co-localization of GFP-positive cell bodies with TdTomato expression (arrows). (G) In projection regions (IO) TdTomato signal presented a punctuated pattern without GFP expression, suggesting that it corresponded to axonal terminals of transduced neurons. Scale bar F,G: 33 µm

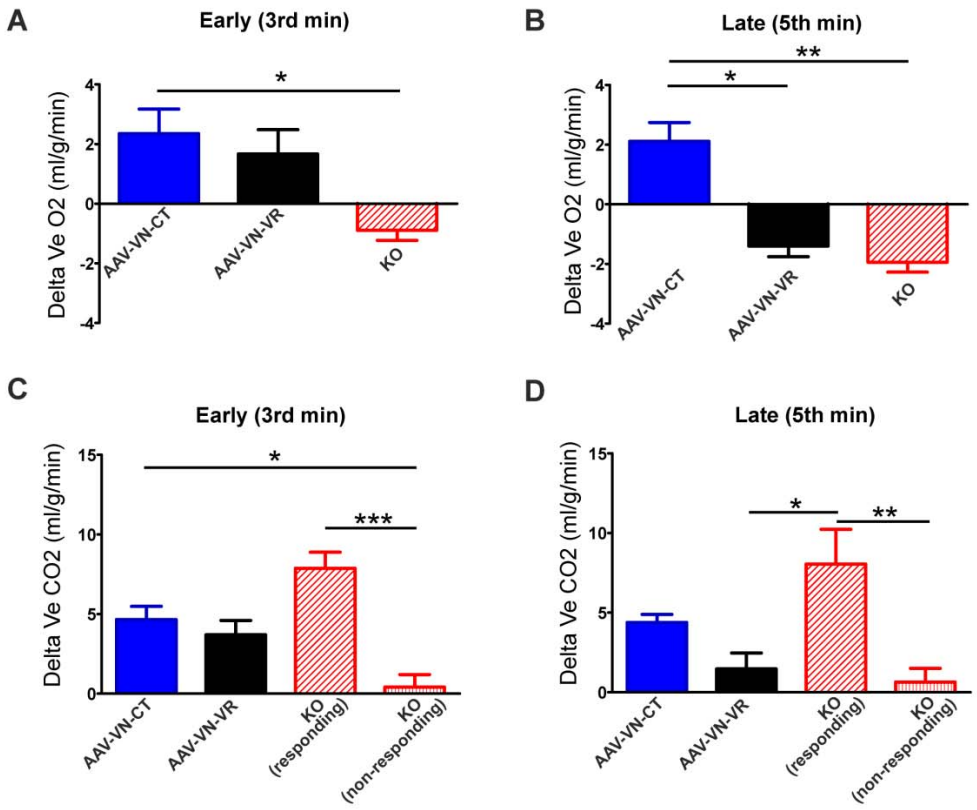

Supplementary Figure 4. Changes in breathing pattern in response to hypoxia or hypercapnia.

(A,B) Early (3rd minute, A) and late (5th minute, B) changes in breathing of AAV-VN-CT (n=14), AAV-VN-VR (n=3) and KO (n=10) mice exposed to 5-min hypoxia (10% O_2). * p<0.05, ** p<0.01 vs CT mice (One-way ANOVA, Tukey post-hoc test).(C,D) Early (3rd minute, A) and late (5th minute, B) changes in breathing of AAV-VN-CT (n=14) ,AAV-VN-VR (n=3) and both responding and non-responding KO (n=5 each) mice exposed to 5 minute hypercapnia (5% CO_2). * p<0.05, ** p<0.01 vs CT mice (One-way ANOVA, Tukey post-hoc test).

Genotype	n	Stage	Stimulus	Delta Ve ($ml.g^{-1}.min^{-1}$)	
				3^{rd} min.	5^{th} min.
CT	6	3 neonates; 3 adults	High CO_2	3.4 ± 1.5	2.9 ± 0.8
KO	6	1 neonate; 5 adults		-0.4 ± 0.4 **	-0.1 ± 0.4 *
KO	7	2 neonates; 5 adults		6.2 ± 1.3 (p=0.1)	7.1 ± 1.7 *

Supplementary Table 1: KO mice exposed to hypercapnia have an abnormal ventilation response.

One group of KO mice (n=6) showed no ventilatory response to CO_2 whereas the second group (n=7) hyperventilated more than CT mice. Thus, overall KO mice had abnormal responses to high levels of CO_2. *: $p<0.05$; **: $p<0.01$ vs CT.